

# Mechanically Stable UV-Crosslinked Polyester-Polycarbonate Solid Polymer Electrolyte for High-Temperature Batteries

Isabell L. Johansson,<sup>[a]</sup> Daniel Brandell,<sup>[a]</sup> and Jonas Mindemark<sup>\*[a]</sup>

Due to the mechanism with which solid polymer electrolytes use to conduct ions, these materials are generally more suitable for high-temperature applications where the ionic conductivity is sufficient and where liquid electrolytes show insufficient stability. To enable high-temperature cycling of polymer electrolytes, the mechanical stability has to be improved. Herein, we report successful long-term cycling of a solid polyester-polycarbonate – poly( $\epsilon$ -caprolactone-co-trimethylene carbonate) (poly(CL-co-TMC)) – electrolyte cross-linked through the addition of multifunctional acrylates and the use of UV-

irradiation, allowing stable cycling of cells for more than 100 cycles at 80 °C, with good rate capabilities ( $0.2 \text{ mAc m}^{-2}$ ) and Coulombic efficiencies exceeding 99%. Both the mechanical properties and the ionic conductivity of the mechanically stabilized poly(CL-co-TMC) were investigated and optimized to reduce the frequency dependence of the moduli while still achieving an acceptable ionic conductivity at elevated temperature. These results indicate that the poly(CL-co-TMC) system can straight-forwardly be modified to allow for higher-temperature applications.

## 1. Introduction

In most modern lithium-ion batteries a liquid electrolyte or a gel electrolyte is utilized, but for applications such as large-scale grid storage and electrified transport, where the safety aspects become critical, solid-state electrolytes become attractive as a means for improving these properties. Solid-state batteries containing solid polymer electrolytes (SPEs) are promising systems, as they are not flammable, will not leak, and are non-toxic. Moreover, SPEs, with high enough modulus remove the need for separators, have a wider electrochemical stability window and offer improved stability vs. lithium metal, which allows battery cells to be constructed with metallic lithium as anode material, thereby giving the battery cells higher energy density.<sup>[1–4]</sup>

The most studied polymeric systems for solid-state batteries are based on poly(ethylene oxide) (PEO), but much research is also being done on alternative polymer systems with attractive properties which PEO lacks, such as amorphicity and high transference numbers.<sup>[3,5–8]</sup> Recent introductions of carbonyl-coordinating polymers such as poly(ethylene carbonate) (PEC),<sup>[9–11]</sup> poly(trimethylene glycol carbonate) (PTEC),<sup>[12]</sup> and

more<sup>[5]</sup> have resolved some of the issues of the PEO-based electrolyte systems. Recent studies within our group have, for example, been conducted on the fully amorphous copolymer poly( $\epsilon$ -caprolactone-co-trimethylene carbonate) (poly(CL-co-TMC)), which shows both good ionic conductivity at ambient temperature and high lithium transference number.<sup>[13]</sup>

While improvements in ionic conductivity have indeed been obtained with this new generation of polymer electrolytes, the ionic conductivity is still poor compared to liquid and gel electrolytes. Most efforts have been directed towards improving the conductivity of SPEs close to 25 °C, i.e., in the working temperature range of liquid-electrolyte cells. Alternatively, these SPEs can be employed in high-temperature applications where their properties are better suitable. The ionic conductivity in a polymer electrolyte is related to the segmental motion of the polymer chains. Therefore, sufficient conductivity for high-rate operation is attained at higher temperatures for SPEs whereas liquid electrolytes under these operational conditions show insufficient stability.<sup>[4,14–17]</sup> However, high temperature introduces a new problem for these polymeric system. While the movement of the polymer chains and the ionic conductivity increases with increased temperature, the material also becomes softer. This leads to mechanical failure, allowing short-circuits and dendrite formation to occur. This inverse relationship between mechanics and conductivity is inherent to the ion conduction mechanism of polymer electrolytes<sup>[18]</sup> and requires specific strategies to circumvent.

There are many methods available to improve the mechanical properties of a polymer electrolyte without seriously compromising their conductive properties, such as increasing the molecular weight of the polymer,<sup>[19]</sup> copolymerization with a mechanically robust block,<sup>[20,21]</sup> addition of nanoparticles,<sup>[22–25]</sup> and cross-linking.<sup>[26–31]</sup> By improving the mechanical stability,

[a] I. L. Johansson, Prof. D. Brandell, Dr. J. Mindemark

Department of Chemistry – Ångström Laboratory  
Uppsala University, Box 538, SE-751 21 Uppsala, Sweden  
E-mail: jonas.mindemark@kemi.uu.se

 Supporting information for this article is available on the WWW under  
<https://doi.org/10.1002/batt.201900228>

 An invited contribution to a Special Collection on Electrolytes for Electrochemical Energy Storage

 © 2020 The Authors. Published by Wiley-VCH Verlag GmbH & Co. KGaA. This is an open access article under the terms of the Creative Commons Attribution Non-Commercial License, which permits use, distribution and reproduction in any medium, provided the original work is properly cited and is not used for commercial purposes.

long-term cycling will be possible. Cross-linking introduces covalent bonds within a polymer, hampers the flow of polymer chains and therefore prevents short-circuits from happening. Mechanically stabilizing the electrode–electrolyte interface should also have a limiting effect on interfacial degradation and interphase formation.

There are many different ways to cross-link polymers for use as polymer electrolytes: by incorporating moieties which are capable of forming cross-links in the polymer chain,<sup>[32]</sup> either along the backbone or in side groups,<sup>[33–35]</sup> by gamma irradiation,<sup>[27]</sup> or by the addition of crosslinking agents.<sup>[26,28,36,37]</sup> Depending on the chemistry chosen, the resulting product might be a covalently cross-linked polymer or a (semi-)interpenetrating network, but for the function of a polymer electrolyte, the specific chemistry behind the mechanical robustness is generally not important for the function of the battery cell.

In this study, a solid polymer electrolyte material with good ionic conductivity at room temperature was mechanically stabilized by utilizing both a two-armed and a three-armed acrylate cross-linking agent. We show that cross-linking by UV-irradiation can be used to achieve good mechanical stability while retaining good ionic conductivity, allowing cycling of battery cells at 80 °C, thereby enabling rate capabilities of 1 C (0.2 mA cm<sup>-2</sup>) and long-term cycling at C/2 with specific discharge capacities around 150 mAh g<sup>-1</sup> for an LiFePO<sub>4</sub>-based half-cell.

## 2. Results and Discussion

In the ring-opening polymerization of ε-caprolactone catalyzed by stannous 2-ethylhexanoate, the end polymer product may be modified by addition of cyclic comonomers. With the addition of 20 mol% of trimethylene carbonate, the resulting random copolymer (structure shown in Figure 1) has shown great utility as a host electrolyte material for Li batteries.<sup>[13]</sup> The poly(CL-co-TMC) material is fully amorphous when LiTFSI is dissolved in it, has a low  $T_g$ , and can support sufficient Li<sup>+</sup> conductivity to be used to cycle batteries at room temperature.<sup>[13]</sup> It is, however, the low  $T_g$  that presents a challenge due to the inverse correlation between mechanical properties and ionic conductivity in conventional SPEs. The material cannot be used at high temperatures due to

insufficient mechanical properties,<sup>[27]</sup> although a higher temperature would further increase the ionic conductivity to enable cycling at high rates.

### 2.1. Crosslinking and Rheology

Utilization at elevated temperatures thus requires mechanically stabilizing the material, e.g. through cross-linking. We have previously shown how this can be accomplished through γ-irradiation.<sup>[27]</sup> However, a much faster and more facile method of cross-linking is by UV-irradiation. By the addition of acrylate cross-linking agents and a UV initiator, both pure poly(trimethylene carbonate) and copolymers with ε-caprolactone have previously been cross-linked using such cross-linking chemistries.<sup>[38]</sup> Here, the trifunctional trimethylolpropane triacrylate (TMPTA) and the difunctional 1,4-butanediol diacrylate (BDA) were used as the cross-linking agents (Figure 1) together with the UV initiator 2,2-dimethoxy-2-phenylacetophenone (DMPA). All polymer films were transparent and homogenous to the eye for all compositions investigated, and there was no significant difference in  $T_g$  for the different compositions, according to DSC measurements (Figure S1). With 5 min of irradiation, there is a noticeable difference in tackiness and color of the pristine and cross-linked films, where the cross-linked polymer films are yellowish and easier to handle.

Because long irradiation times might cause degradation of the polymer, which would have a detrimental effect on cycling, irradiation of the polymer films was limited to 2–5 min. Figure S2 shows the change in moduli when the polymer is exposed to UV irradiation for different lengths of time; there is an obvious change in appearance already after 2 min, and little difference between 2 min and 5 min. However, the cross-linking efficiency is affected by the sample thickness, and to err on the side of caution, and ensure thorough cross-linking throughout the entire electrolyte films, an irradiation time of 5 min was selected. During extended UV irradiation, i.e., 30 min, there is an evident decrease in the moduli, likely an effect of chain scission. The successful cross-linking was confirmed by rheological measurements; here, a frequency-independent  $G'$  suggests covalent cross-linking and rubber-like properties, while a dominant  $G''$  at low frequencies would indicate that the material will flow and deform over time. As can be seen in the frequency sweeps on electrolyte films containing 20 wt% LiTFSI in Figure 2, the storage modulus ( $G'$ ) is higher than the loss modulus ( $G''$ ) for all samples within the investigated frequency range. This is also the case for the pristine sample, but the frequency dependence of the moduli is significantly reduced in the cross-linked samples. The absence of a crossover indicates that the cross-linked solid polymer electrolyte is mechanically stable at 25 °C within the measurement range, and able to withstand mechanical loads during operation of the battery cell. This is also true for the sample which has not been cross-linked. However, at low concentrations of the cross-linking agents (< 5 wt% for TMPTA and < 10 wt% for BDA),  $G'$  and  $G''$  show frequency dependencies indicating that the liquid-like properties of the sample are increasing and a crossover might

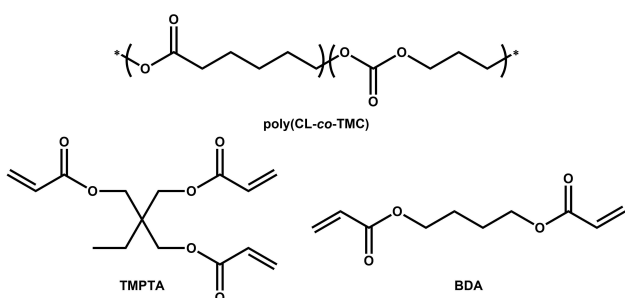
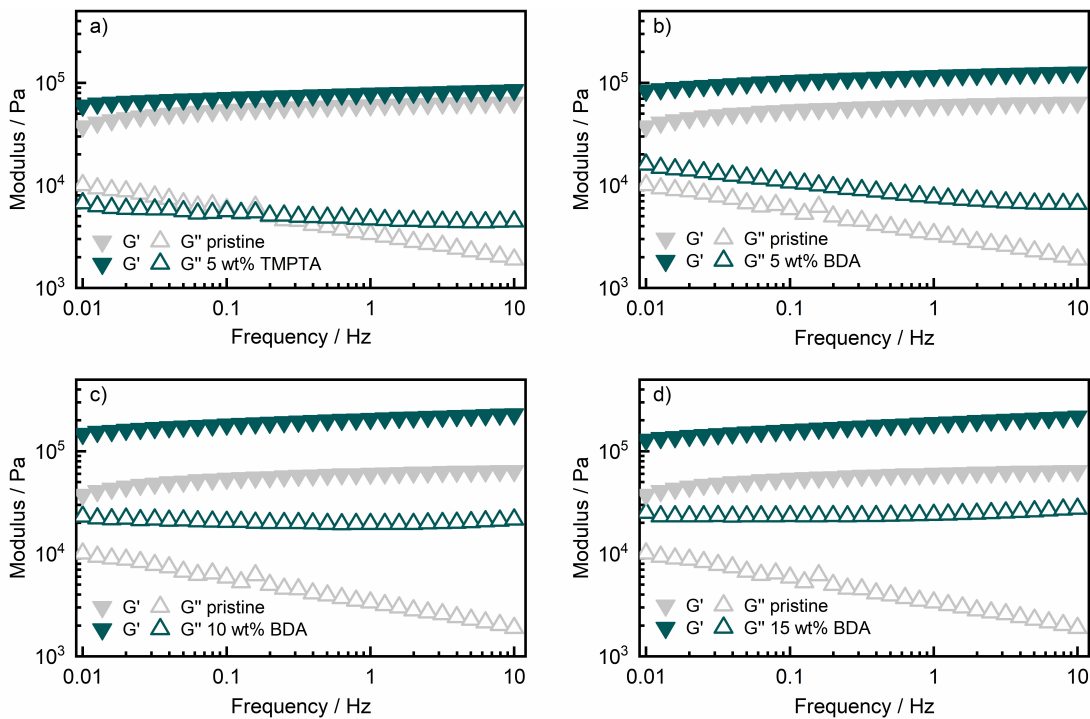


Figure 1. The copolymer poly(CL-co-TMC), trimethylolpropane triacrylate (TMPTA) and 1,4-butanediol diacrylate (BDA).



**Figure 2.** Rheological measurements on poly(CL-co-TMC) with a) 5 wt% TMPTA, b) 5 wt% BDA, c) 10 wt% BDA, and d) 15 wt% BDA shown in green symbols. A pristine non-cross-linked film is shown in grey symbols as reference. Measurements were performed at 25 °C. All films contain 20 wt% LiTFSI and all cross-linked films contain 5 wt% DMPA.

occur at very low frequencies.<sup>[27]</sup> In contrast, the samples cross-linked with 5 wt% TMPTA or 10–15 wt% BDA show diminished frequency dependencies of the moduli, typical of a covalently cross-linked material.

At the same concentration of cross-linking agent (Figure 2a–b), the trifunctional TMPTA gives a similar storage modulus as the difunctional BDA. A noteworthy difference can be seen in the loss modulus where the TMPTA gives an improved stability and lower value compared to all investigated concentrations of BDA, indicating a higher degree of cross-linking with TMPTA compared to BDA. As the  $T_g$  is determined by the chain mobility, an increase in  $T_g$  was expected for the cross-linked SPEs; however, no significant differences can be seen for the different sample compositions in DSC measurements (Figure S1). Since the ionic conductivity of polymer electrolytes is directly linked to the chain mobility of the polymer host, it follows that it can be anticipated that the cross-linking would also have no major effect on the ionic conductivity. Additionally, increasing the amount of cross-linking agent (Figure 2b–d) causes an increase in modulus and reduces the frequency dependence of the loss modulus, also due to an increase in cross-linking density. This effect appears to become saturated somewhere between 10 and 15 wt% BDA, as increasing the amount of BDA beyond 10 wt% does not lead to substantial changes in the rheological response.

At higher temperatures, the effect of the cross-linking becomes more noticeable. In Figure 3 the comparison between a pristine and a sample cross-linked with 10 wt% BDA is shown. At 100 °C a crossover between  $G'$  and  $G''$  is clearly seen for the

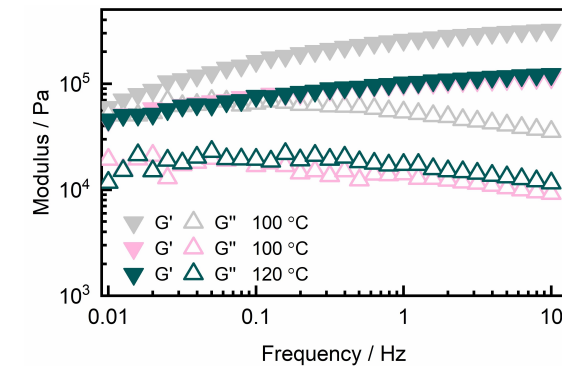


**Figure 3.** Rheology measurements on poly(CL-co-TMC) at elevated temperature. A non-cross-linked film containing 20 wt% LiTFSI is shown in grey symbols. Cross-linked films, containing 20 wt% LiTFSI, 5 wt% DMPA, 10 wt% BDA, is shown in pink (100 °C) and green (120 °C) symbols.

pristine sample, which indicates that the sample is behaving more like a liquid than a solid at frequencies below this point; meanwhile, this is not seen for the cross-linked sample, which shows clear solid-like properties even at 120 °C. Additionally, the modulus of the cross-linked film shows little temperature dependence, with only a slight increase of the loss modulus when the temperature is increased.

The total ionic conductivity, as obtained from electrochemical impedance spectroscopy, can be seen in Figure 4. In the cross-linked samples, it was found that irradiation for longer than 5 min had little to no effect on the ionic conductivity (Figure 4a). This is in contrast with what was seen

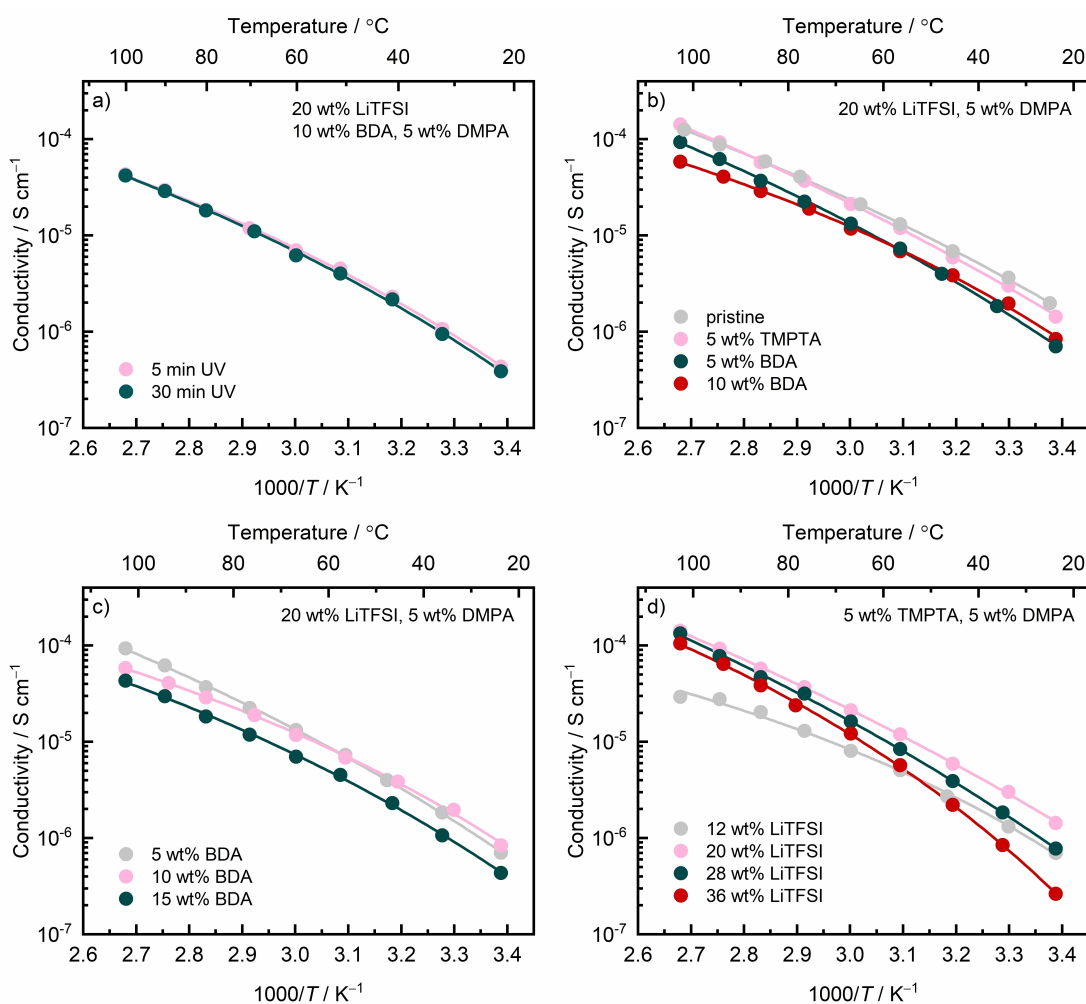


**Figure 4.** Ionic conductivity measurements of a) films with different irradiation time, b) pristine polymer film and cross-linked films with different cross-linking agents, c) cross-linked polymer films with BDA at different concentrations, and d) cross-linked polymer films with different concentrations of LiTFSI. Pristine films contain only 20 wt% LiTFSI. With the exception of in a), all electrolyte films were irradiated for 5 min. The lines represent VFT fits.

for  $\gamma$ -irradiated samples, where a higher irradiation dose resulted in lower ionic conductivity, implying anion degradation.<sup>[27]</sup> Irradiation for shorter than 5 min might not be sufficient to achieve maximum crosslinking density for a certain amount of additives, while excessive irradiation is expected to cause chain scission, which results in an increase in the number of mobile chain ends which would be anticipated to be manifested as an increase in ionic conductivity. Since there is a balance between the effects of increased mobility by chain scission, lowered mobility by cross-linking and lowering of the salt concentration due to anion degradation, these effects are not individually distinguishable from the ionic conductivity data alone.

Compared to the non-cross-linked (pristine) sample, the films cross-linked with BDA and TMPTA showed somewhat lower ionic conductivity (see Figure 4b). The ionic conductivity was also found to decrease with increasing amounts of the cross-linking agent (Figure 4c). The combined data from results from the rheological measurements and impedance measurements indicate that good mechanical stability can be obtained

without severely sacrificing the conductivity using either 10 wt% of the two-armed cross-linking agent BDA or 5 wt% of the three-armed TMPTA; further increasing the amount of cross-linking agent would only have a negative impact on the ionic conductivity.

Finally, the correlation between the amount of LiTFSI and the ionic conductivity in the system cross-linked with 5 wt% TMPTA is shown in Figure 4d, and the maximum in ionic conductivity is found at 20 wt% LiTFSI.

## 2.2. Battery Cycling

Battery cells for cycling were prepared by sandwiching electrolyte films between a Li metal anode and a LiFePO<sub>4</sub> cathode. The cathode was prepared using non-cross-linked poly(CL-co-TMC) as binder, to provide ionic connectivity within the porous structure and to provide an ionically conducting interface between the SPE and the cathode. Because the cross-linked samples have lower ionic conductivity than the pristine

samples, but better mechanical properties at elevated temperature, the cycling performance is expected to be inferior for the cross-linked samples at low to moderate temperatures. As seen in Figure 5, when cells containing the different electrolytes were cycled at 1C from room temperature up to 100 °C, we find that the cell containing the electrolyte cross-linked with 10 wt% BDA consistently shows discharge capacities that are higher than for the cell containing the electrolyte cross-linked with 5 wt% TMPTA, which exhibits low specific discharge capacities at all temperatures, see also Figure S3a. Since the electrolyte cross-linked with TMPTA does not display a lower ionic conductivity than the other electrolytes (Figure 4), the low discharge capacities cannot be attributed to bulk ion transport. It is possible that this is instead related to interfacial ion transport between the electrolyte film and the poly(CL-co-TMC) ion-conducting binder within the electrode. Similar limitations by interfacial ion transport have previously been noted in related SPE systems.<sup>[39,40]</sup>

Although the cell containing the pristine sample did not short-circuit in this experiment, instead persisting until 100 °C, cells comprising this electrolyte show much more unreliable performance with a tendency to short-circuit. This is illustrated in Figure S3b and Figure S6; during these experiments, the pristine sample short-circuited during the rest period at 40 °C. While cycling at up to 80 °C is possible for some samples, we also observe unreliable performance with poor coulombic efficiencies and cell failure after a limited number of cycles (Figure S6).

Typically, the pristine SPE material has shown good cycling capability at room temperature, but fails at high C-rates, such as those in Figure 5. To show the rate capability of the cross-linked SPE when cycled under conditions where SPEs have a more notable advantage over liquid electrolytes, a C-rate test was performed on an SPE cross-linked with BDA at 80 °C, see Figure 6. The cycling rate was increased from C/10 up to 10C, at which the cell no longer showed any significant capacity,

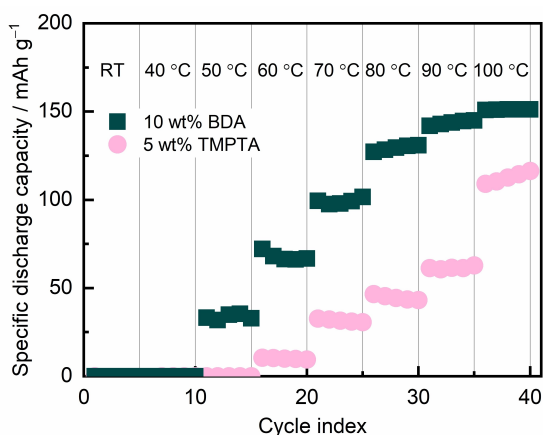


**Figure 5.** Cycling of Li | SPE | LiFePO<sub>4</sub> cells, containing either a pristine polymer electrolyte or polymer electrolytes cross-linked with either TMPTA or BDA, at 1 C ( $0.29 \text{ mA cm}^{-2}$ ) from room temperature up to 100 °C. Following a 5 h rest the cells were allowed to perform five cycles at each temperature, and the temperature was increased by 10 °C every 12 h.

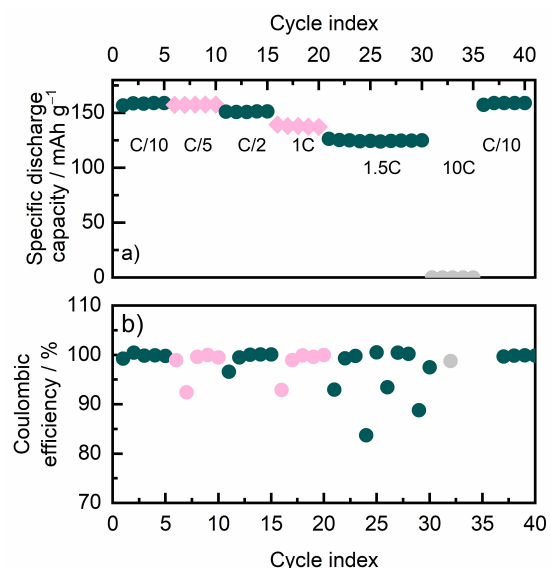


**Figure 6.** Cycling performance of poly(CL-co-TMC)-based cells a) at different C-rates at 80 °C and b) the Coulombic efficiency. The polymer film contains 20 wt% LiTFSI and is cross-linked with 5 wt% DMPA and 10 wt% BDA. 1 C is equivalent to a current density of  $0.28 \text{ mA cm}^{-2}$ .

followed by the cycling rate being decreased back to C/10 to see if and how the cell was affected by the rapid cycling. The rapid cycling did not seem to have an effect on the cell, which was able to regain the same specific capacity which it had during the initial five cycles. At 1.5C the cycling becomes less stable, as can be seen in the fluctuating values for the coulombic efficiency at this cycling rate and low coulombic efficiency for cycles following the first at each increased C-rate, cycling curves for 1.5 C and C/10 can be seen in Figure S5. The fastest cycling rate possible with stable cycling was 1C but, as expected, there is a small penalty in the discharge capacity at this cycling rate. At C/10 and C/5 the discharge capacity is around  $160 \text{ mAh g}^{-1}$ , and drops to  $140 \text{ mAh g}^{-1}$  at 1C. Long-term galvanostatic cycling was performed on a cell containing a SPE cross-linked with 10 wt% BDA at 80 °C, which shows stable cycling for more than two months and 100 cycles at a cycling rate of C/2 (Figure 7). The gradual increase in specific capacity seen during the first cycles is likely caused by limitations in the interfacial contact between the cathode and the SPE. Although this has been noted in other SPE systems previously,<sup>[39]</sup> it is typically not observed for poly(CL-co-TMC) electrolytes<sup>[13]</sup> (such as in the cell containing the non-cross-linked electrolyte cycled at 80 °C in Figure S6). Here, the high C-rate likely exacerbates the issue for the cross-linked material by making any limitations in ionic connectivity more critical for the overall capacity utilization. Gradual improvement of the electrode-electrolyte interface during extended cycling at 80 °C thus leads to the initial capacity improvements seen in Figure 7a.

Few authors report cycling data of cross-linked SPE systems where both high cycling rate and high temperature is utilized during cycling, making comparison with other systems difficult. While the cross-linked poly(CL-co-TMC) system has too low

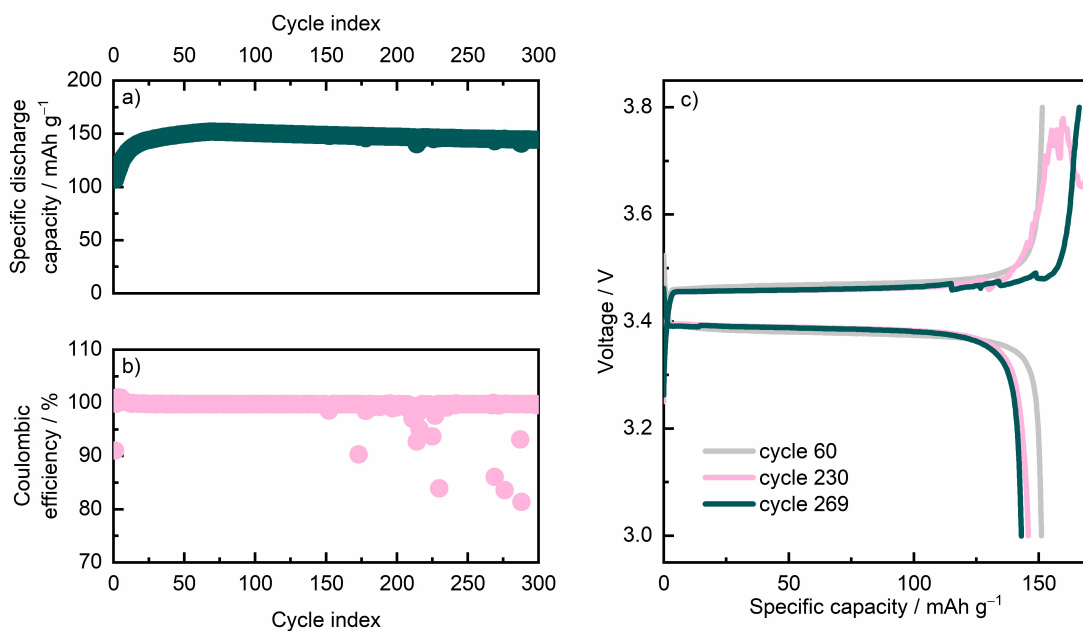


**Figure 7.** a) Long-term (two months) cycling, with b) Coulombic efficiency, and c) charge-discharge curves of a normal cycle (grey) and two outliers (pink and green), of LiFePO<sub>4</sub>-based half-cells containing poly(CL-co-TMC) polymer electrolyte with 20 wt% LiTFSI, 5 wt% DMPA, and 10 wt% BDA, at 80 °C and C/2 (0.16 mA cm<sup>-2</sup>).

ionic conductivity to cycle at high rates at room temperature, unlike some cross-linked PEO/glyme systems,<sup>[29]</sup> it has a lower overpotential compared to PEO systems at a similar cycling temperature and higher cycling rate.<sup>[36,41]</sup> After 150 cycles the SPE starts showing some instability which is most likely due to side-reactions occurring as the battery is charging, see Figure 7c. The instability might be caused by the potential cut-off values (3.0–3.8 V), where poly(CL-co-TMC) might be unstable due to the additives and high temperature. LSV measurements on pristine and cross-linked SPE, Figure S4, show minor oxidation reactions starting at 3.5 V, with an ultimate oxidation limit at ~4.2 V at 80 °C and no tangible difference between the cross-linked and the pristine material. Despite the anodic current observed between 3.5–4.2 V, the material is obviously sufficiently stable at potentials up to 3.8 V when cycling vs. LiFePO<sub>4</sub> to sustain stable long-term cycling. However, the cycling behavior of the UV-irradiated cells is more stable and has less erratic voltage profiles compared to gamma-irradiated cells.<sup>[27]</sup> While these data already show that the cross-linked electrolyte allows for improved performance with higher discharge rates compared to the non-cross-linked system, with further optimization of the system, such as adjusting the potential window, employing other salts, and allowing the cell to cycle at a slower rate during the first couple of cycles to form stable interfaces, the long-term cycling behavior of the cross-linked system is expected to be stabilized further.

### 3. Conclusions

In contrast to the often futile quest for low-temperature performance in SPEs, an alternative approach is to instead

utilize the notable electrochemical stability and performance at elevated temperatures. This, however, requires mechanical stability in combination with high molecular flexibility, an apparent oxymoron that needs to be specifically addressed. In this paper, we have demonstrated that polyester/polycarbonate SPEs cross-linked with UV-irradiation and cross-linking agents can achieve long-term stable cycling at temperatures up to 80 °C. The cross-linked SPEs have excellent mechanical properties, good ionic conductivity, and are able to cycle for long periods of time at temperatures where the behavior of the non-cross-linked material is unreliable and prone to short-circuit. The cross-linked polymer electrolytes show high rate capability and stable cycling behavior for well over 100 cycles at elevated temperatures. Instabilities during further cycling might be caused by unoptimized voltage cut-off potentials during cycling. The employed UV-crosslinking method could easily be applied to other solid polymer electrolyte systems which suffer from poor mechanical properties, and improve the reliability of the polymer electrolyte, resulting in more stable battery cycling behavior.

### Experimental Section

**Materials:** Poly(CL-co-TMC) was synthesized through ring-opening polymerization of ε-caprolactone and trimethylene carbonate catalyzed by tin(II) 2-ethylhexanoate as described previously.<sup>[42,43]</sup> Trimethylolpropane triacrylate (TMPTA, ABCR), 1,4-butanediol diacrylate (BDA, Aldrich) and 2,2-dimethoxy-2-phenylacetophenone (DMPA, Sigma-Aldrich) were stored in a glove box under argon and used as received. Lithium bis(trifluoromethylsulfonyl)imide (LiTFSI, Solvionic) was dried at 120 °C for 24 h in vacuum before use.

**Electrolyte preparation:** To prepare the polymer electrolyte films, poly(CL-co-TMC), LiTFSI, DMPA, and TMPTA or BDA were dissolved in acetonitrile. Of the total electrolyte mass, the salt content was varied between 12 and 36 wt%, and the cross-linking agent content was varied between 1 and 15 wt%. Films were prepared in PTFE molds by controlled solvent evaporation,<sup>[42]</sup> followed by UV-irradiation under a 365 nm, 4×9 W UV lamp. The irradiation time was varied between 0 and 30 min.

**Mechanical characterization:** Mechanical characterization was performed using oscillatory frequency sweeps on a TA Instruments AR 2000 with an 8 mm aluminum parallel plate geometry. The frequency sweeps were performed at a controlled strain of 0.5%, from 0.01 to 10 Hz, at a controlled normal force of  $1.0 \pm 0.1$  N at 25 °C. Calibration of the rheometer and measurements were performed under nitrogen gas flow.

**Ionic conductivity:** The SPEs were sandwiched between two stainless steel blocking electrodes in CR2032 type coin cells. The thickness of the SPEs was the average of at least three different measurements using a digital indicator (Mitutoyo). The impedance response was recorded for frequencies 1 to 10 MHz at a 10 mV amplitude using a Schlumberger SI 1260 Impedance/Gain-phase Analyzer instrument. Prior to measurements, the cells were heated to 100 °C for 1 h, and then allowed to cool down to room temperature overnight, to ensure good interfacial contact between the SPE and the stainless steel electrodes. The measurements were carried out at room temperature, and at every 10 °C interval between 30 and 100 °C. Conductivity was calculated using the bulk resistance, which was gained by fitting the data to a Debye equivalent circuit in ZView.

**Cycling:** Galvanostatic cycling tests were carried out with an ARBIN BT-2043 on lab-scale cells. Coin cells were assembled with an SPE film placed between a Li metal anode and a LiFePO<sub>4</sub> (LFP) cathode. Galvanostatic cycling was performed at C-rates based on a theoretical capacity of 170 mAh g<sup>-1</sup>. Cathodes were prepared by ball-milling 70 wt% LFP powder (Phostech, P2 nanosized), 15 wt% carbon powder (C65, Imerys), and 15 wt% poly(CL-co-TMC) as binder dissolved in acetonitrile (for 0.150 g binder, 4 mL of acetonitrile was used), and the mixture was coated using a 150 µm doctor blade on carbon-coated aluminum foil.

## Acknowledgements

The authors acknowledge funding from the European Research Council (grant number 771777 FUN POLYSTORE).

**Keywords:** solid polymer electrolyte · mechanical stabilisation · ionic conductivity · rheology · Li battery

- [1] W. Xu, J. Wang, F. Ding, X. Chen, E. Nasybulin, Y. Zhang, J. G. Zhang, *Energy Environ. Sci.* **2014**, *7*, 513.
- [2] M. Armand, J. M. Tarascon, *Nature* **2008**, *451*, 652.
- [3] E. Quararone, P. Mustarelli, *Chem. Soc. Rev.* **2011**, *40*, 2525.
- [4] C. Xu, G. Hernández, S. Abbrent, L. Kobera, R. Konefal, J. Brus, K. Edström, D. Brandell, J. Mindemark, *ACS Appl. Energy Mater.* **2019**, *2*, 4925.
- [5] J. Mindemark, M. J. Lacey, T. Bowden, D. Brandell, *Prog. Polym. Sci.* **2018**, *81*, 114.
- [6] M. M. Doeffer, L. Edman, S. E. Sloop, J. Kerr, L. C. De Jonghe, *J. Power Sources* **2000**, *89*, 227.

- [7] T. K. Lee, N. F. M. Zaini, N. N. Mobarak, N. H. Hassan, S. A. M. Noor, S. Mamat, K. S. Loh, K. H. KuBulat, M. S. Su'ait, A. Ahmad, *Electrochim. Acta* **2019**, *316*, 283.
- [8] O. Buriez, Y. B. Han, J. Hou, J. B. Kerr, J. Qiao, S. E. Sloop, M. Tian, S. Wang, *J. Power Sources* **2000**, *89*, 149.
- [9] K. Kimura, M. Yajima, Y. Tominaga, *Electrochim. Commun.* **2016**, *66*, 46.
- [10] J. Zhang, J. Yang, T. Dong, M. Zhang, J. Chai, S. Dong, T. Wu, X. Zhou, G. Cui, *Small* **2018**, *14*, 1.
- [11] T. Morioka, K. Nakano, Y. Tominaga, *Macromol. Rapid Commun.* **2017**, *38*, 1.
- [12] W. He, Z. Cui, X. Liu, Y. Cui, J. Chai, X. Zhou, Z. Liu, G. Cui, *Electrochim. Acta* **2017**, *225*, 151.
- [13] J. Mindemark, B. Sun, E. Törmä, D. Brandell, *J. Power Sources* **2015**, *298*, 166.
- [14] K. Smith, M. Earleywine, E. Wood, J. Neubauer, A. Pesaran, *SAE [Tech. Pap.]* **2012**.
- [15] Q. Hu, S. Osswald, R. Daniel, Y. Zhu, S. Wesel, L. Ortiz, D. R. Sadoway, *J. Power Sources* **2011**, *196*, 5604.
- [16] K. Q. He, J. W. Zha, P. Du, S. H. S. Cheng, C. Liu, Z. M. Dang, R. K. Y. Li, *Dalton Trans.* **2019**, *48*, 3263.
- [17] R. Genieser, M. Loveridge, R. Bhagat, *J. Power Sources* **2018**, *386*, 85–95.
- [18] J. F. Snyder, R. H. Carter, E. D. Wetzel, *Chem. Mater.* **2007**, *19*, 3793.
- [19] F. Harun, C. H. Chan, Q. Guo, *Macromol. Symp.* **2017**, *376*, 1700040.
- [20] W. S. Young, W. F. Kuan, T. H. Epps, *J. Polym. Sci. Part B* **2014**, *52*, 1.
- [21] A. Bergfelt, M. J. Lacey, J. Hedman, C. Sångeland, D. Brandell, T. Bowden, *RSC Adv.* **2018**, *8*, 16716.
- [22] S. Choudhury, R. Mangal, A. Agrawal, L. A. Archer, *Nat. Commun.* **2015**, *6*, 1.
- [23] N. Lago, O. Garcia-Calvo, J. M. Lopezdelamo, T. Rojo, M. Armand, *ChemSusChem* **2015**, *8*, 3039.
- [24] C. Wang, Y. Yang, X. Liu, H. Zhong, H. Xu, Z. Xu, H. Shao, F. Ding, *ACS Appl. Mater. Interfaces* **2017**, *9*, 13694.
- [25] T. Eriksson, J. Mindemark, M. Yue, D. Brandell, *Electrochim. Acta* **2019**, *300*, 489.
- [26] L. Porcarelli, C. Gerbaldi, F. Bella, J. R. Nair, *Sci. Rep.* **2016**, *6*, 1.
- [27] J. Mindemark, A. Sobkowiak, G. Oltean, D. Brandell, T. Gustafsson, *Electrochim. Acta* **2017**, *230*, 189.
- [28] R. Khurana, J. L. Schaefer, L. A. Archer, G. W. Coates, *J. Am. Chem. Soc.* **2014**, *136*, 7395.
- [29] M. Falco, C. Simari, C. Ferrara, J. R. Nair, G. Meligrana, F. Bella, I. Nicotera, P. Mustarelli, M. Winter, C. Gerbaldi, *Langmuir* **2019**, *35*, 8210.
- [30] S. Tan, S. Walus, J. Hilborn, T. Gustafsson, D. Brandell, *Electrochim. Commun.* **2010**, *12*, 1498.
- [31] B. Sun, I. Y. Liao, S. Tan, T. Bowden, D. Brandell, *J. Power Sources* **2013**, *238*, 435.
- [32] Z. Zhang, D. Sherlock, R. West, R. West, K. Amine, L. J. Lyons, *Macromolecules* **2003**, *36*, 9176.
- [33] J. Mindemark, L. Imholt, J. Montero, D. Brandell, *J. Polym. Sci. Part A* **2016**, *54*, 2128.
- [34] J. Mindemark, L. Imholt, D. Brandell, *Electrochim. Acta* **2015**, *175*, 247.
- [35] A. Nishimoto, K. Agehara, N. Furuya, T. Watanabe, M. Watanabe, *Macromolecules* **1999**, *32*, 1541.
- [36] H. Ben Youcef, O. Garcia-Calvo, N. Lago, S. Devaraj, M. Armand, *Electrochim. Acta* **2016**, *220*, 587.
- [37] J. Jiang, H. Pan, W. Lin, W. Tu, H. Zhang, *Mater. Chem. Phys.* **2019**, *236*, 121781.
- [38] E. Bat, B. H. M. Kothman, G. A. Higuera, C. A. van Blitterswijk, J. Feijen, D. W. Grijpma, *Biomaterials* **2010**, *31*, 8696.
- [39] B. Sun, J. Mindemark, K. Edström, D. Brandell, *Electrochim. Commun.* **2015**, *52*, 71.
- [40] A. Bergfelt, G. Hernández, R. Mogensen, M. J. Lacey, J. Mindemark, D. Brandell, T. M. Bowden, *ACS Appl. Polym. Mater.* **2020**.
- [41] I. Villaluenga, S. Inceoglu, X. Jiang, X. C. Chen, M. Chintapalli, D. R. Wang, D. Devaux, N. P. Balsara, *Macromolecules* **2017**, *50*, 1998.
- [42] J. Mindemark, E. Törmä, B. Sun, D. Brandell, *Polymer* **2015**, *63*, 91.
- [43] A. P. Pégo, A. A. Poot, D. W. Grijpma, J. Feijen, *J. Mater. Sci. Mater. Med.* **2003**, *14*, 767.

Manuscript received: December 28, 2019  
 Version of record online: March 6, 2020